

Adaptive Energy Diffusion for Blind Inverse Halftoning

Lei Wang¹, Binh-Son Hua², and Xueqing Li¹

¹ College of Computer Science, Shandong University
wanglpqq@gmail.com, xqli@sdu.edu.cn

² School of Computing, National University of Singapore
huabinhs@comp.nus.edu.sg

Abstract. We propose a blind inverse halftoning method with adaptive energy diffusion. A discrete Voronoi diagram is built by treating halftone dots as Voronoi cell sites. Gaussian filters are then created adaptively based on Voronoi cells and used for energy diffusion to form the grayscale inverse halftone image. We further perform a median filter on the Gaussian filters' parameters to maintain consistency of filters across different image regions. To remove artifacts in dense halftone dots area, we show that a secondary Voronoi diagram can be built based on the non-halftone dots and a heuristic blending can be employed. Comparing with other inverse halftoning methods, our method is able to remove artifacts in both sparse and dense halftone dots regions and produces visually pleasant gray-scale images. Our method is also applicable to edge enhancement and structure-aware halftoning.

Keywords: digital halftoning, inverse halftoning, error diffusion, discrete Voronoi diagram.

1 Introduction

Digital halftoning [1,2], the transformation from continuous tone images into images with limited gray level such as binary ones, has been widely used in publishing applications, such as newspapers, books, magazines, etc. However, halftone images are typically difficult to manipulate. Many image processing and operations, such as scaling, enhancement and rotation are hard to impose to halftone images. In order to impose these operations on those images, continuous tone images need to be reconstructed from halftone images through the technique of inverse halftoning. Inverse halftoning has been popularly used to halftone image manipulation, conversion, and compression. There is no clear model or unique algorithm for inverse method because there are different halftoning algorithms according to different models. So the halftoning process is a many-to-one mapping. In our research, an adaptive weighted filtering technique is proposed to solve the inverse halftoning problem.

Concerning halftoning methods [3], error diffusion [1,2] and dot diffusion [4] are known as two typical ones. There are also edge enhancement halftoning

methods such as structure-aware halftoning [5] and edge enhancement error diffusion [6]. For traditional error diffusion method, there are also various different methods according to the differences of diffusion kernels such as Floyd method [1], Jarvis method [2], Ostromoukhov method [7].

According to analysis existed methods, the inverse halftoning algorithms can be classified into three categories. The first class treats inverse halftoning as a denoising problem which removes the high frequency noise occurred from the halftoning process. A simple example of this category is low pass filtering. However, low pass filtering tends to produce blurred images. There are other more sophisticated methods to reduce blur and sharpen edges such as fast blind inverse halftoning [8], wavelet-based methods [9,10], fast inverse halftoning for error diffused halftones [11] and nonlinear filtering [12]. This class of algorithm is less computational demanding, but some of them may blur the edge or only be suitable for some particular types of halftone images. The second class treats the inverse halftoning as an image reconstruction problem. A lot of traditional inverse problem methods are used to solve this problem, e.g., MMSE and MAP projection based method [13], Projection onto Convex Set (POCS) [14]. These methods can usually give estimated images with good visual quality, but they usually require some special conditions or computationally intensive. For example, some of them assume the availability of the halftone kernel which is only used in error diffusion halftone method. The third category is learning-based method which uses training set or machine learning to get the continuous tone image. Look Up Table based method (LUT) [15] and decision tree learning [16] based method belong to this class. Especially for LUT based method, there are a lot of extended algorithms to improve the execution efficiency, like tree-structured LUT [18], edge based LUT [17]. Basically, the training method can be used to different halftoning methods. However, this class algorithm needs some training sets to get the solution.

Our method belongs to the first category and performs inverse halftoning in a completely different approach. Using the Voronoi diagram, we formulate adaptive Gaussian filters to distribute energy from Voronoi diagram sites to image pixels. We further perform a median filter on the Gaussian filters' parameters to maintain consistency of filters across different image regions. To remove artifacts in dense halftone dots area, we show that a secondary Voronoi diagram can be built based on the non-halftone dots and a heuristic blending can be employed.

This paper is organized as follows. Section 2 describes how adaptive Gaussian filters are formed by using Voronoi diagram. We then describe the blending of two inverse halftone images in order to remove artifacts in section 3. Implementation and experiment details are given in section 4. Finally, conclusion is given in section 5.

2 Adaptive Energy Diffusion

2.1 Voronoi Diagram Construction

Voronoi diagram is a well known space partition method in the space of different distance metric. Given an open set Ω , a set of n different sites (or seeds) S_i ,

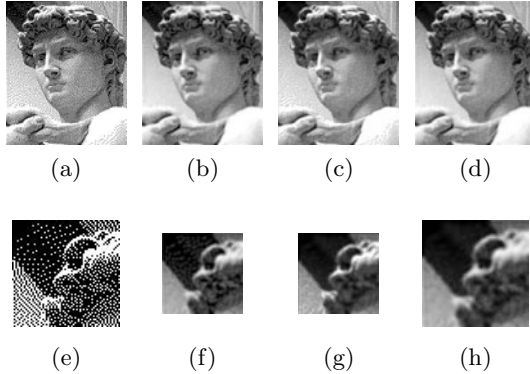


Fig. 1. (a) David halftone by Floyd error diffusion. (b) Inverse halftone using black Voronoi diagram. (c) Inverse halftone using white Voronoi diagram. (d) Inverse halftone using black and white blending scheme. (e) Enlarged the top left 64×64 patch of (a). (f) Enlarged the top left 64×64 patch of (b). (g) Enlarged the top left 64×64 patch of (c). (h) Enlarged the top left 64×64 patch of (d).

$i = 1..n$, and a distance function d , the Voronoi diagram (or cell) is defined as n distinct subsets (cells) C_i such that:

$$C_i = \{\omega \in \Omega \mid d(\omega, S_i) < d(\omega, S_j), \text{ for } i, j = 1..n, j \neq i\} \quad (1)$$

Our method starts by computing the discrete Voronoi diagram from the input halftone image H . Notice that Voronoi sites can be halftone dots or non-halftone dots in the halftone image. To explain easily and clearly, we refer halftone dots as black dots and non-halftone dots as white dots. Consequently, there are two possible Voronoi diagram from a halftone image. In the next section, the images employ black dots as Voronoi sites is defined as the black version and is notated with a subscript b , while others employ white dots as Voronoi sites named white version and notated with a subscript w . Every step in our method is the same in both black and white version of the Voronoi diagrams. So here we will only describe our method based on the black version of the Voronoi diagram.

In order to avoid dense halftone regions that contains too many black dots that may result in distorted discrete Voronoi diagram, we first redistribute the dots to a larger image H' of which size is a blown up scale factor λ of the original halftone image size. For every black dot location (x, y) , we redistribute according to the following scheme:

$$H'(\lambda x, \lambda y) = \lambda^2 H(x, y) \quad (2)$$

Notice that the energy in the halftone image is scaled up by λ^2 so that the mean energy of H and H' is kept similar. Then the discrete Voronoi diagram is formed on the redistributed halftone image H' . Here we use Jump Flooding Algorithm on GPU [19] to compute the discrete Voronoi diagram from H' . An example of the redistributed halftone H' and its Voronoi diagram is shown in Figure 2.

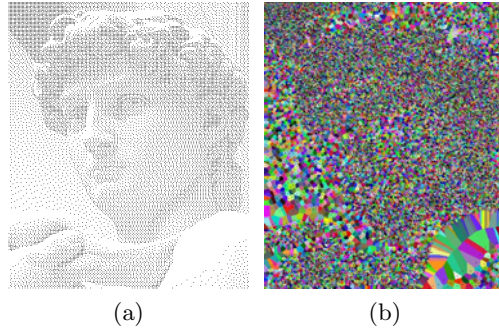


Fig. 2. The redistributed halftone, and its black Voronoi diagram ($\lambda = 2$)

Further processing steps will be performed on this blown up image size. We only downsample to the original halftone image size at the final step which produces the grayscale image of the original size.

2.2 Gaussian Filter Design

After Voronoi diagram is constructed, inverse halftoning can be viewed as an energy diffusion process. Each black dot, which is a Voronoi site, diffuses its energy to its local neighborhood that is defined by the Voronoi cell it belongs to. In other words, the black dots diffuse energy as far as possible until reaching another black dot's neighborhood. Consequently, this forms an adaptive energy diffusion scheme.

In order to achieve smooth energy diffusion, Gaussian distribution is employed. Each black dot is the center of a Gaussian filter which diffuses energy into its Voronoi cell following an isotropic Gaussian distribution. The diffusion process is controlled by the energy conservation constraint in each Voronoi cell. This allows us to conserve the local tone in the inverse halftone image. Mathematically, the constraint can be written in the following equation.

$$\sum_{(x,y) \in C_i} I'(x,y) = \lambda^2 \quad (3)$$

This constraint is easily implemented by a normalization stage after Gaussian energy diffusion.

Next, we show how a Gaussian filter can be designed adaptively for each Voronoi site. The Gaussian filter should diffuse most of its energy inside the Voronoi cell. Furthermore, we observe that 95% of the energy diffused by an isotropic Gaussian filter lies in the radius of 3σ where σ is the standard deviation of the Gaussian function. Consequently, σ should be adaptively determined according to the Voronoi cell where the filter is located. From σ , we then easily set the radius of the isotropic filter to be 3σ .

Let C_i be a Voronoi cell and a be its discrete area value. The standard deviation σ of the Gaussian filter in C_i is determined by the following equation:

$$\sigma = (\log(1 + a))^k \quad (4)$$

where k is set to 1.3. The intuition behind the above equation is that σ should be small in small Voronoi cell, and gets larger in larger cells to further diffuse energy. Our experiments show that σ varies logarithmically to the area of Voronoi cell, thus the above equation is used.

In order to further smoothen the energy diffusion process, we constrain that the σ parameters should vary smoothly among Voronoi cells. This constraint is implemented by a median filter after σ is calculated for each Voronoi cell. At the end of this step, Gaussian filter parameter σ for every Voronoi cell is computed. We are now ready for the energy diffusion.

2.3 Isotropic Gaussian Energy Diffusion

Given Gaussian filter for each Voronoi cell, the energy diffusion process is stated as below.

$$I'_b(x, y) = \exp\left(\frac{(x - x_0)^2 + (y - y_0)^2}{2\sigma^2}\right) \quad (5)$$

where $(x, y) \in C_i$ and (x_0, y_0) is the corresponding Voronoi site. After energy diffusion is performed for every Voronoi cell, a normalization stage is run to ensure the total energy in each Voronoi cell equal to λ^2 so that the local tone is conserved.

3 Black and White Versions Blending

Recall that in the Voronoi diagram construction stage, there are two possibilities to form the Voronoi diagram, V_b and V_w , which lead to two different inverse halftone images, I'_b and I'_w . The grayscale intensity of the inverse halftone image can be computed as follow, depending on which version of the Voronoi diagram is used.

$$I'(x, y) = \begin{cases} \lambda^2 - I'_b(x, y) & \text{for black Voronoi Diagram} \\ I'_w(x, y) & \text{for white Voronoi diagram} \end{cases} \quad (6)$$

The black inverse halftone image has smooth energy diffusion in regions where the black dots are sparsely distributed. However, in regions where the black dot density is high, σ becomes very small and artifacts appeared. But high density of black dots means low density of white dots, therefore, we can make use of the corresponding region in the white inverse halftone image to correct those artifacts. The blending scheme is then defined as follow.

$$I'(x, y) = \begin{cases} \lambda^2 - I'_b(x, y) & \text{if } d(x, y) \leq \tau \\ I'_w(x, y) & \text{otherwise} \end{cases} \quad (7)$$

where $d(x, y)$ returns the density of Voronoi sites in the (x, y) location; τ is a threshold set by user.

Finally, the inverse halftone image I is easily computed by downsampling I' by a factor of λ . We summarize stages of our method in the following table.

Algorithm 1. Blind Inverse Halftoning using Voronoi Diagram

Step 1. Redistribute black dots into a larger image which is scaled by λ from the original halftone image size.

Step 2. Construct two discrete Voronoi diagrams, V_b and V_w , by treating black dots and white dots as sites, respectively.

Step 3. For each Voronoi diagram, compute standard deviation σ for every Voronoi cell.

Step 4. For each Voronoi diagram, perform a median filter on σ of Voronoi cells.

Step 5. Compute energy diffusion I'_b and I'_w respectively for Voronoi diagram V_b and V_w .

Step 6. Compute grayscale intensity I' by blending two versions of black I'_b and white I'_w .

Step 7. Downsample I' to obtain the final grayscale image I .

4 Results

In our implementation, the scale factor λ is set to 6. Discrete Voronoi diagram is computed on an NVIDIA GeForce 8600 GTS graphics card using OpenGL and



Fig. 3. Lena halftone by Floyd error diffusion

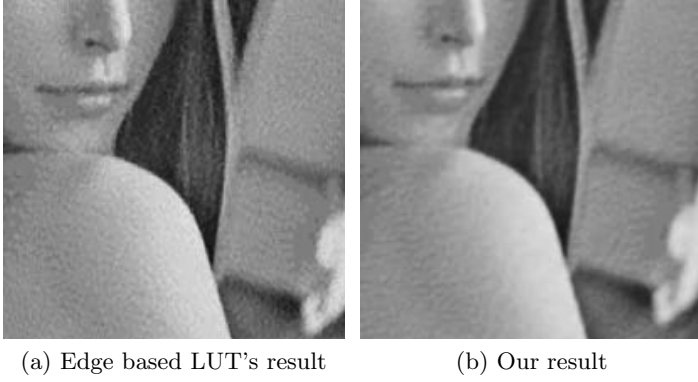


Fig. 4. Zoom-in of the Lena example

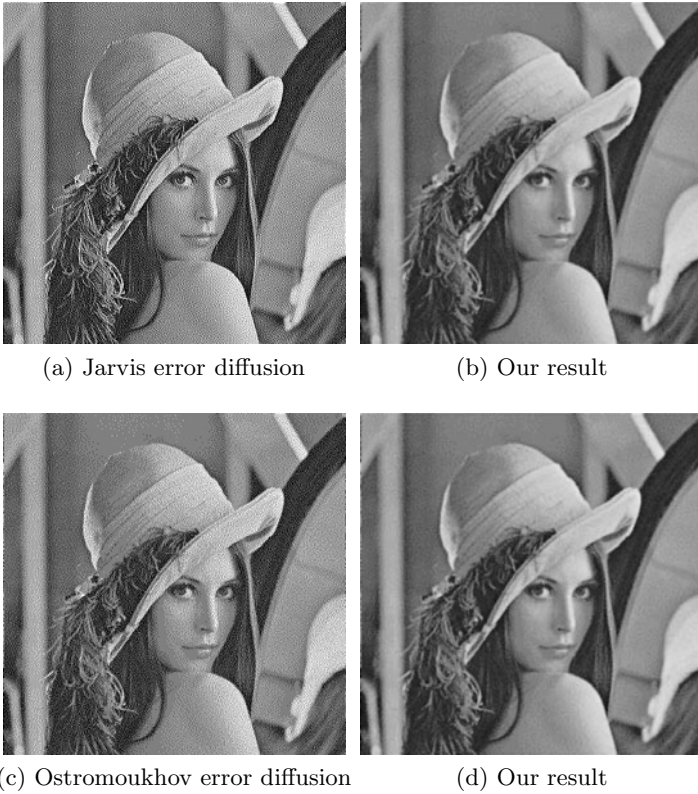


Fig. 5. Lena halftone by other error diffusion methods and our inverse halftoning results

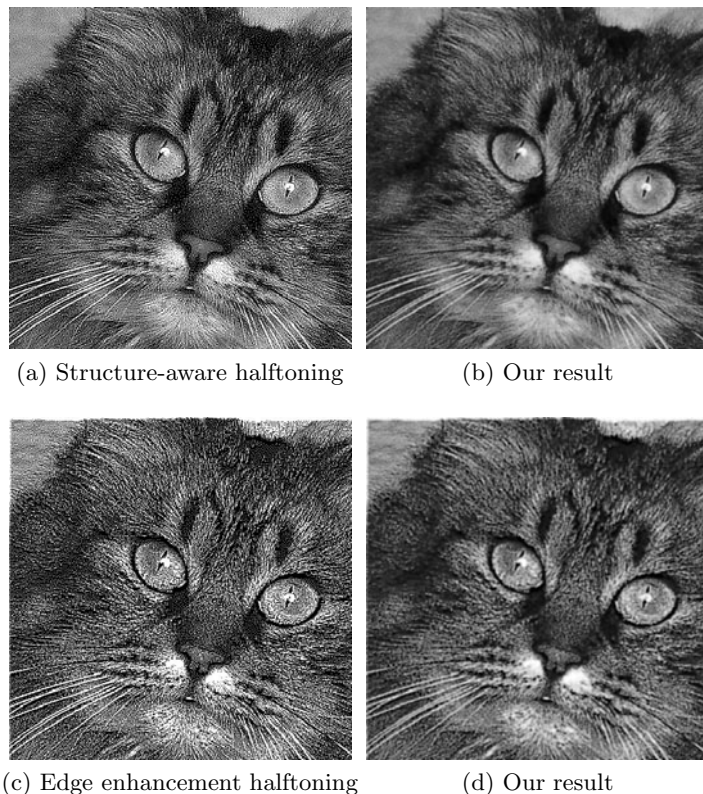


Fig. 6. Cat example by structure-aware halftoning and edge enhancement halftoning, and our inverse halftoning results

Cg shading language. Other steps of our method are implemented on CPU. We compare our results with inverse halftoning methods designed for error diffusion, and with those that can be used with any halftoning methods. The David example is obtained from Wikipedia. The Cat example is from the structure-aware halftoning paper [5].

Figure 1 shows the inverse halftoning of the David example. We see that black Voronoi diagram produces visually pleasant result. However, at the top left 64×64 patch of the halftone image, the number of black dots are so dense that it leads to artifacts in the inverse grayscale images. Those artifacts do not appear in the inverse grayscale produced by the white Voronoi diagram. Therefore, the blending result produces the most visually pleasant grayscale image.

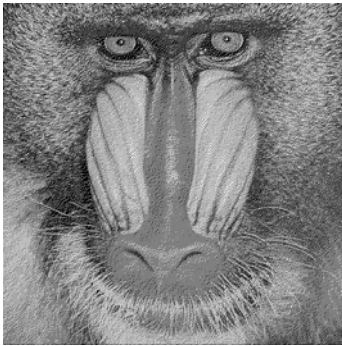
We further compare our method with other inverse halftoning methods based on the popular Lena example. Figure 3 shows the comparison of our method with LUT [15], edge based LUT [17] and fast filter method [11]. In this example, the Lena halftone image is produced by Floyd error diffusion method; the parameter



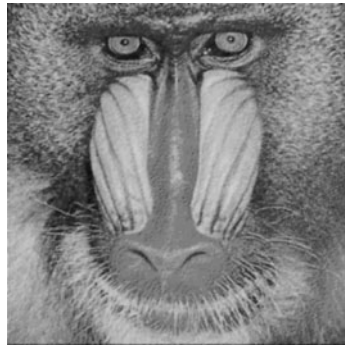
(a) Boat image floyd halftoning



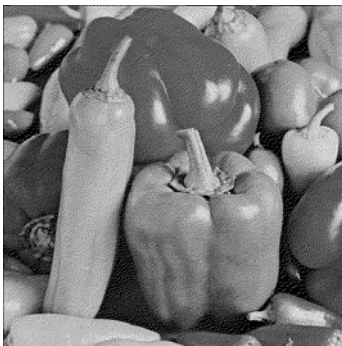
(b) Our result



(c) Mandrill image floyd halftoning



(d) Our result



(e) Peppers image floyd halftoning



(f) Our result

Fig. 7. Different images example by floyd halftoning and our inverse halftoning results

λ is 4 and threshold τ is 0.6. Figure 4 further shows an zoom-in patch in the Lena example. In addition, Figure 7 show some other images example with the same parameters.

Additionally, our method works with any error diffusion method. Figure 5a and Figure 5b show the Jarvis error diffusion halftone image [2] and our result of inverse halftoning. Figure 5c and Figure 5d show Ostromoukhov error diffusion halftone image [7] and our corresponding result. We adopted the same parameters as the above Floyd error diffusion example.

Our method is also robust to edge enhancement [6] or structure-aware halftoning [5] method. Figure 6 show the results of our algorithm for edge enhanced halftoning methods. In this example, λ is set to 6 and τ is set 0.7.

5 Conclusion

In this paper, a blind inverse halftoning method is proposed based on Voronoi diagram and adaptive Gaussian energy diffusion. Our inverse halftoning method is independent of halftoning methods used to produce the input halftone image so it can be applied to any halftone images without any prior knowledge. Our method also resolves artifacts occurred in too dense regions by making use of two Voronoi diagrams at the same time.

Future directions include optimization for the computation of σ parameters of Gaussian filters in order to minimize artifacts after energy diffusion. We also investigated in anisotropic Gaussian filter to further constrain and preserve edges in the inverse halftoning results.

Acknowledgments. The authors would like to thank Dr. Kok-Lim Low for his ideas and comments in this project. This work was done when Lei Wang was an intern in National University of Singapore.

References

1. Floyd, R.W., Stienberg, L.: An Adaptive Algorithm for Spatial Grayscale. Proc. SID 17(2), 75–77 (1976)
2. Jarvis, J., Judice, C., Ninke, W.: A survey of techniques for displaying of continuous-tone pictures on bilevel displays. Computer. Graphics Image Process. 5, 130 (1976)
3. Ulichney, R.: Digital Halftoning. MIT Press, Cambridge (1987)
4. Knuth, D.E.: Digital halftones by dot diffusion. ACM Trans. Graph. 6, 245–273 (1987)
5. Pang, W., Qu, Y., Wong, T., Cohen-Or, D., Heng, P.: Structure-aware halftoning. In: ACM SIGGRAPH 2008 Papers, SIGGRAPH 2008, Los Angeles, California, August 11 - 15, pp. 1–8. ACM, New York (2008)
6. Eschbach, R., Knox, K.T.: Error-diffusion algorithm with edge enhancement. J. Opt. Soc. Am. A 8, 1844–1850 (1991)
7. Ostromoukhov, V.: A simple and efficient error-diffusion algorithm. In: Proceedings of the 28th Annual Conference on Computer Graphics and interactive Techniques SIGGRAPH 2001, pp. 567–572. ACM, New York (2001)

8. Venkata, N.D., Kite, T.D., Venkataraman, M., Evans, B.L.: Fast blind inverse halftoning. In: Proc. IEEE International Conference on Image Processing, vol. 2, p. 648 (1998)
9. Luo, J., De Queiroz, R., Fan, Z.: A robust technique for image descreeing based on the wavelet transform. *IEEE Trans. on Signal processing* 46(4), 1179–1184 (1998)
10. Xiong, Z., Orchard, M.T., Ramchandran, K.: Inverse halftoning using wavelets. In: Proc. IEEE International Conference on Image Processing, pp. 569–572 (1996)
11. Kite, T.D., Venkata, N.D., Evans, B.L., Bovik, A.C.: A high quality, fast inverse halftoning algorithm for error diffusion halftones. In: Proc. IEEE International Conference on Image Processing, vol. 2, p. 593 (1998)
12. Shen, M.Y., Kuo, C.-C.J.: A Robust Nonlinear Filtering Approach to Inverse Halftoning. *J. Vis. Commun. Image Represen.* 12, 845 (2001)
13. Stevenson, R.L.: Inverse halftoning via MAP estimation. *IEEE Trans. on Image Process.* 6, 574–583 (1997)
14. Bozkurt Unal, G., Cetin, A.E.: Restoration of Error-Diffused Images Using Projection Onto Convex Sets. *IEEE Trans. on Image Processing* (2001)
15. Mese, M., Vaidyanathan, P.P.: Look Up Table (LUT) Method for Inverse Halftoning. *IEEE Trans. on Image Process.* 10(10), 1566–1578 (2001)
16. Kim, H.Y., de Queiroz, R.: Inverse halftoning by decision tree learning. In: Proc. IEEE Int. Conf. Image Processing, vol. 2, pp. 913–916 (2003)
17. Chung, K.L., Wu, S.T.: Inverse Halftoning Algorithm Using Edge-Based Lookup Table Approach. *IEEE Trans. on Image Process.* 14(10), 1583–1589 (2005)
18. Mese, M., Vaidynathan, P.P.: Tree-Structured Method for LUT Inverse Halftoning and for Image Halftoning. *IEEE T. Image Processing* 11(6), 644–655 (2002)
19. Rong, G., Tan, T.S.: Variants of jump flooding algorithm for computing discrete voronoi diagrams. In: *ISVD 2007: Proceedings of the 4th Int. Symp. on Voronoi Diagrams in Science and Engineering*, pp. 176–181. IEEE Computer Society, Los Alamitos (2007)